applied optics

Calibration of a CubeSat spectroradiometer with a narrow-band widely tunable radiance source

STEVEN VAN DEN BERG,[1,2] PAUL DEKKER,[1,*] GERARD OTTER,[3] MARCELA PELICA PÁSCOA,[3] AND NIELS DIJKHUIZEN[3]

[1]VSL Dutch Metrology Institute, Thijsseweg 11, 2629 JA, Delft, The Netherlands
[2]Currently at The Hague University of Applied Sciences, Rotterdamseweg 137, 2628 AL, Delft, The Netherlands
[3]TNO, Stieltjesweg 1, 2628 CK Delft, The Netherlands
*Corresponding author: pdekker@vsl.nl

Received 11 December 2020; revised 30 January 2021; accepted 1 February 2021; posted 3 February 2021 (Doc. ID 417467); published 26 February 2021

We have developed an SI-traceable narrow-band tunable radiance source based on an optical parametric oscillator (OPO) and an integrating sphere for the calibration of spectroradiometers. The source is calibrated with a reference detector over the ultraviolet/visible spectral range with an uncertainty of <1%. As a case study, a CubeSat spectroradiometer has been calibrated for radiance over its operating range from 370 nm to 480 nm. To validate the results, the instrument has also been calibrated with a traditional setup based on a diffuser and an FEL lamp. Both routes show good agreement within the combined measurement uncertainty. The OPO-based approach could be an interesting alternative to the traditional method, not only because of reduced measurement uncertainty, but also because it directly allows for wavelength calibration and characterization of the instrumental spectral response function and stray light effects, which could reduce calibration time and cost.

https://doi.org/10.1364/AO.417467

1. INTRODUCTION

In today's world, satellite instruments provide an essential basis for a vast amount of information that is utilized not only in a wide range of scientific applications but also in our daily lives. Among other fields, the physical quantities derived from satellite observations are of interest in atmospheric physics and geoscience. While on ground the physical quantities of interest can often be measured directly, this is usually not possible for space-based remote sensing. In this case, a satellite instrument detects the reflection or emission of radiation from the Earth's surface or atmosphere, from which the required physical quantities are then retrieved. As the basic physical principle is set by the interaction of radiation with the Earth's atmosphere and surface (radiative transfer), the use of radiances and their respective units is often preferred within retrieval methods. Here, the relevant units are $\mathrm{W\,m^{-2}\,sr^{-1}}$ for radiance and $\mathrm{W\,m^{-2}\,sr^{-1}\,nm^{-1}}$ for spectral radiance.

To quantify and possibly reduce the uncertainty on the physical quantities to be retrieved, the requirements on the calibration of the measurement instrument get more and more demanding. As a consequence, the calibration requirements on the on-ground equipment used for calibrating and characterization of the Earth observation instrumentation get increasingly tight as well. Moreover, traceability to the international system of units (SI) is important in space-based observation, since SI traceability is a prerequisite for comparability of data records acquired over a long time interval (decades) and with different instruments. Comparability of long-term data records is essential for monitoring of a wide range of essential climate variables (ECVs) that have been adopted by the United Nations Framework Convention on Climate Change. Quantitative measurement of many of these ECVs relies on spectrally resolved optical measurements with calibrated spectroradiometers.

The current state of the art for radiance responsivity calibration of spectroradiometers is the use of an FEL lamp with a calibrated diffuser or a calibrated integrating sphere. The advantage of these sources is their broadband (white light) output, so that the entire spectral range can be illuminated at once. The disadvantages of these sources is that they are omnidirectional and that the spectral content is much wider than usually needed. Only a small fraction of the light is emitted within the field of view and spectral range of the spectroradiometer to be calibrated, and additional measures to suppress stray light may be needed. Moreover, additional measurements are required with specialized narrow-band sources to further characterize the instrument. Other disadvantages are the limited lifetime of the calibration of the FEL lamp in terms of burning hours and its low emission in the UV wavelength range.

In this paper, we present the application of a narrow-band tunable radiance source for the calibration of spectroradiometers. Such sources have been shown to be an interesting alternative to lamp-based sources, as e.g., demonstrated for the calibration of spectral (ir-)radiance responsivity of detectors [1]. The radiance source is obtained by coupling monochromatic light from an optical parametric oscillator (OPO) into an integrating sphere. The source is calibrated with a calibrated reference detector in combination with several geometrical measurements. With this method, spectral selection thus takes place at the source, which means that a radiometric calibration of a satellite instrument needs to be carried out with a wavelength scan. As a demonstration of the calibration method, a CubeSat spectroradiometer (TROPOLITE, TNO [2]) has been calibrated in the ultraviolet/visible (UV/VIS) wavelength range with this source. For comparison and validation of the method, the spectroradiometer has also been calibrated with a radiance source based on an FEL lamp and a diffuser. First we will describe the calibration method, the setup, and the calibration of the radiance source itself, including a discussion on the uncertainty budget. In the second part of the paper, the calibration of the CubeSat spectroradiometer with both methods is presented. The results of this comparison and the associated measurement uncertainties will be discussed.

2. CALIBRATION METHOD AND MEASUREMENT MODEL

A spectroradiometer under test is calibrated against the known radiance of a reference source. The reference radiance source consists of an integrating sphere with a well-defined aperture and an OPO, providing narrow-band tunable light. Other design details, such as the radiance level as compared to radiance levels from the Earth's atmosphere can be found in [3]. To account for instability of the light source, the flux within the sphere is measured with a monitor detector mounted in one of the sphere output ports. The radiance of the source is calibrated by measuring the flux with a calibrated reference detector, positioned at a distance d from the sphere aperture. The transfer of the flux from the radiance source to the reference detector is determined by the geometry of the system: the radius of the source aperture r_s, radius of the detector aperture r_d, and distance d between both apertures, as shown in Fig. 1. For round apertures of the source and reference detector, the radiance of the source $L(\lambda)$ is given by

$$L(\lambda) = \frac{i_{\mathrm{ref}}}{R(\lambda)} \frac{1}{\pi^2 r_s^2 f}, \tag{1}$$

where $R(\lambda)$ is the spectral responsivity of the reference detector and i_{ref} the net current measured with the reference detector. The parameter f is defined as

$$f = 2\frac{r_d^2}{(r_s^2 + r_d^2 + d^2) + \sqrt{\left((r_s^2 + r_d^2 + d^2)^2 - 4r_s^2 r_d^2\right)}} \tag{2}$$

(see, e.g., [4]).

Simultaneously, the current from the monitor detector is measured. The calibration thus links the monitor detector

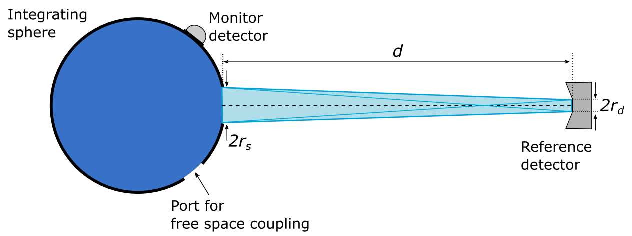

Fig. 1. Schematic of integrating sphere and reference detector with relevant geometrical parameters.

response to a known radiance level from the source aperture. We will refer to this as the "effective spectral radiance responsivity" of the monitor detector [unit: $\mathrm{A/(W\,m^{-2}sr^{-1})}$], which is given by

$$R_{\mathrm{rad,mon}} = \frac{i_{\mathrm{mon,cal}}}{L(\lambda)}, \tag{3}$$

where $i_{\mathrm{mon,cal}}$ is the net current (i.e., corrected for dark current), as measured during calibration. The wavelength dependence of $R_{\mathrm{rad,mon}}$ is measured as a function of wavelength by tuning the OPO.

The currents from both the reference detector and the monitor detector are measured with an electrometer in charge-accumulation mode, which has been shown to be a suitable method to measure detector currents generated with pulsed light sources [1]. The current is determined from the charge accumulated in a registered time interval. Once the effective radiance responsivity has been determined through calibration, the monitor detector current can be used as a measure for the radiance of the sphere aperture. Traceability to SI units thus comprises both radiometric and geometrical standards (see [3] for an extended traceability chart).

3. CALIBRATION SETUP

An overview of the calibration setup is shown in Fig. 2. As a light source, an OPO is used (Ekspla NT 242), which emits light pulses with a pulse length of 3 ns to 6 ns at a repetition rate of 1 kHz. The wavelength of the OPO system can be tuned from 210 nm to 2600 nm, which is achieved by using the signal or idler wavelength directly, or by second harmonic generation and sum frequency generation of the signal and idler. The emitted pulse energy ranges from about 10 μJ to 500 μJ over its tuning range. The system contains a spectral cleaning unit for pure single wavelength emission. The line width is $< 8\ \mathrm{cm^{-1}}$. A laser spectrum analyzer is available to verify the OPO wavelength.

The light is coupled into the integrating sphere through free space. Since the OPO output is strongly wavelength dependent, the optical power sent into the integrating sphere is controlled with a variable attenuator, being a filter wheel with various neutral density (ND) filters. The integrating sphere has a diameter of 30 cm and is coated with Spectralon. A 50 mm diameter precision aperture defines the emitting area of the sphere. The estimated coherence length corresponding to the OPO line width is roughly 2 mm, which is much smaller than the typical path length propagated in the integrating sphere (several meters). Due to the short coherence length, no speckle is observed from the sphere aperture. The integrating sphere

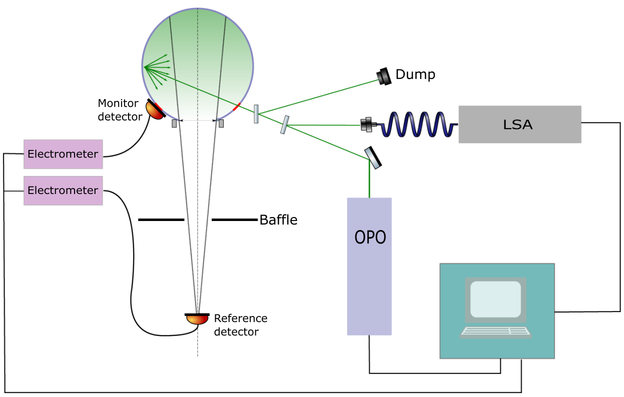

Fig. 2. Schematic of tunable radiance source. OPO, optical parametric oscillator; LSA, laser spectrum analyzer.

is equipped with a silicon photodiode as the monitor detector, covering the UV/VIS wavelength range.

As a reference detector, we use a trap detector with an aperture of 6 mm diameter, which consists of three silicon photodiodes in a trap configuration [5]. The trap detector is one of VSL's primary references for the UV/VIS wavelength range and has been calibrated for spectral responsivity against the absolute cryogenic radiometer of VSL. The diameters of the apertures of both the integrating sphere and reference detector have been measured at VSL with a coordinate measurement machine. The distance between the source and detector aperture is measured with a calibrated tubular-inside micrometer. A baffle with a diameter of about 40 mm is positioned in between the sphere and the reference detector for stray light reduction. The photocurrents from both the monitor detector and reference detector are measured with two identical electrometers (Keithley 6514). The variable attenuator is set such that the accumulated charge in a measurement interval of 50 s is less than 20 μC, which is the maximum charge that can be measured with the instrument. The electrometer used to measure the current from the reference detector has been calibrated by the VSL Electricity group. Data acquisition takes place by setting the OPO wavelength and subsequently triggering the measurements with both electrometers.

4. RADIANCE SOURCE CALIBRATION

We have calibrated the radiance source in the UV/VIS wavelength range. For this measurement, the reference detector is positioned at 500 mm from the sphere aperture. Although the OPO and detectors allow for a much wider tuning range, we focus on the measurement range from 370 nm to 480 nm, which is the operating range of the TROPOLITE spectroradiometer that will be calibrated. Calibration takes place by tuning the OPO in steps of 10 nm. No attenuation was used for 370 nm to 400 nm. The attenuator was set at a nominal transmission of $10^{-2.5}$ for 410 nm to 480 nm, since the OPO output peaks in this wavelength range. Before data acquisition starts, the wavelength is set, and the capacitors of the electrometers are discharged. During the measurement, the accumulated charge is stored with a time stamp in the buffer of the electrometer every 0.5 s. Each measurement consists of 100 datapoints. To account for stray light and dark current as measured by the reference detector, an additional measurement is performed with the stray light baffle closed, while light is emitted from the sphere aperture. Furthermore, the dark current of the monitor detector is measured with the OPO turned off.

As a check of the method and to estimate residual stray light effects, another calibration of the source is performed at two positions of the reference detector (500 mm and 750 mm) over a spectral range of 250 nm to 950 nm. As described in Section 4.B, additional measurements are performed to determine various contributions to the measurement uncertainty of the calibration.

A. Calibration Results

From the charge measurements and the corresponding time stamps, the average photocurrent is calculated for both detectors. Based on these results, the spectral responsivity of the reference detector, and the geometrical parameters, the effective spectral radiance responsivity of the monitor detector is determined using Eqs. (1)–(3). Here, the net currents are used, i.e., corrected for the stray light and dark measurements as described above. As pointed out earlier, the effective spectral radiance responsivity is defined such that it relates the radiance of the integrating sphere aperture to the average photocurrent of the monitor detector.

Before executing the calibration of the radiance source as described above, we have performed several measurements to verify the linearity of the response of the detectors to determine the appropriate attenuator settings. This was done by measuring the photocurrents at various settings of the attenuator. From these measurements, it is observed that for higher power levels, saturation leads to a nonlinear response of the monitor detector. This is clearly observed in Fig. 3, showing the spectral radiance responsivity of the monitor detector at various attenuation settings. Because of its position in the sphere port, the monitor detector generates a photocurrent that is about one order of magnitude larger compared to the reference detector. For the highest level of attenuation (nominal transmission of $10^{-2.5}$ and 10^{-3}), differences are negligible (<0.05%). For these attenuator settings, both detectors are in the linear operation range. This is visualized in the inset in Fig. 3 for the wavelength range of 410 nm to 480 nm, for which the OPO output is highest (see below). Calibration of the spectral radiance responsivity in this wavelength range has therefore been performed with an attenuated OPO beam to ensure linearity. Subsequent calibrations with the integrating sphere as a reference radiance source have been performed in this way as well.

Compared to a lamp–diffuser-based approach, much higher radiance levels can be obtained with an OPO coupled into an integrating sphere. This is particularly relevant in the UV wavelength range, in which the irradiance from an FEL lamp is very low. In the absence of an attenuator, the maximum radiance level that can be obtained with the OPO setup is shown in Fig. 4. For comparison, we have plotted the typical radiance from a diffuser positioned at 75 cm from a 1000 W FEL lamp, as emitted within a spectral band of 0.5 nm. This is the approximate spectral width (FWHM) of the spectroradiometer that has been investigated in the case study (see Section 5). The radiance within this bandwidth has been estimated by multiplying the spectral radiance

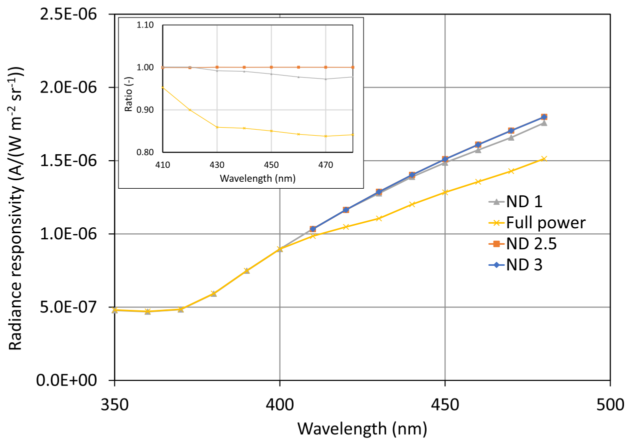

Fig. 3. Measurement of the effective spectral radiance responsivity at various power levels of the OPO beam coupled to the integrating sphere. The power level ranges from full power, to three orders of magnitude attenuation (ND 3). The inset shows the effective spectral radiance responsivity for full power, ND 1, and ND 2.5, normalized to the effective spectral responsivity as measured with ND 3 attenuation.

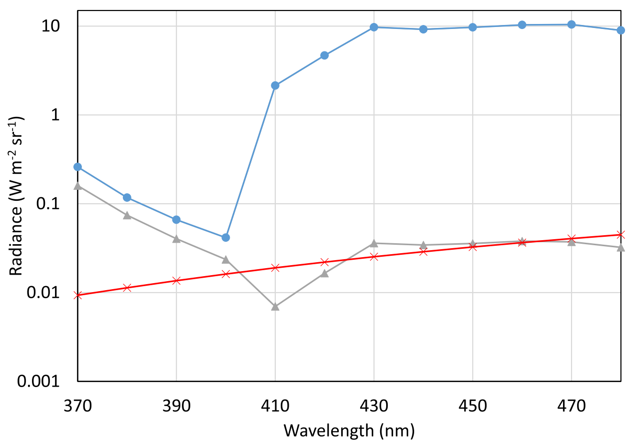

Fig. 4. Radiance from the sphere without attenuation (blue dots). For comparison the (attenuated) radiance level as used for the calibration of the spectroradiometer is shown (gray triangles) as described in Section 5. The red curve (crosses) shows the radiance emitted within a 0.5 nm bandwidth, as obtained with an FEL lamp and a diffuser (Section 5.B).

from the diffuser (expressed in units $\mathrm{W\,m^{-2}\,sr^{-1}\,nm^{-1}}$) by this bandwidth. It may be interesting to note here that the bandwidth of the instrument under test is thus an important parameter when making the trade-off between wideband and narrow-band reference sources for calibration. The third curve in the figure is the (attenuated) radiance level of the integrating sphere fed with the OPO, as used for calibration of the spectroradiometer in the case study. Though only the range for the spectroradiometer under test is shown here, a much wider range (210 nm to 2600 nm) is covered by the OPO.

B. Measurement Uncertainty

The radiance source acts as a reference source for calibration of spectroradiometers. In this section, we quantify the measurement uncertainty assigned to the radiance emitted from the source. We consider a slightly revised version of the measurement equation here:

$$L(\lambda) = \frac{i_{\mathrm{ref}}}{R(\lambda)}\frac{1}{\pi^2 r_s^2 f}\cdot C_{\mathrm{EM}}\cdot C_{\mathrm{stray}}\cdot C_{\mathrm{align}}, \quad (4)$$

in which we introduce the correction factors C_{EM}, C_{stray}, and C_{align}. These factors account for calibration of the electrometer and stray light and alignment effects. From calibration of the electrometer, it is found that $C_{\mathrm{EM}} = 1.0012$. This has been taken into account for determination of the spectral radiance responsivity above. The other correction factors are one, but are included since stray light and alignment effects contribute to the measurement uncertainty.

1. Responsivity of Reference Detector

The reference detector has been calibrated against a cryogenic radiometer using a double monochromator system, which has a finite slit width. The reported responsivity is the responsivity as measured under these conditions, i.e., while illuminated with light having a certain spectral width. For the visible domain, the spectral width is $\Delta = 9$ nm (full base width), and the slit function is approximated with a triangular distribution. The responsivity for a single wavelength with a very narrow bandwidth (tenths of nanometers, as for the OPO) may therefore deviate from the reported value. The bandwidth difference gives rise to a deviation of the responsivity, given by

$$u_{bp}(R) = \frac{2R(\lambda) - R(\lambda-\delta\lambda) - R(\lambda+\delta\lambda)}{\delta\lambda^2} \times \frac{\Delta^2}{12}, \quad (5)$$

where $\delta\lambda = 10$ nm is the wavelength difference between subsequent wavelengths for which the reference detector has been calibrated against the cryogenic radiometer. The responsivity in the UV/blue wavelength range changes in a rather irregular way, leading to deviations due to bandwidth up to 0.1% for 370 nm; for other wavelengths, the deviations are mostly below 0.05%. The deviation is included in the uncertainty budget as standard uncertainty ($k = 1$).

Furthermore, any deviation between the emitted wavelength and the set wavelength of the OPO also contributes to the uncertainty on the responsivity of the detector. The emitted wavelength has been measured with a calibrated laser spectrum analyzer, showing a wavelength deviation below 0.03 nm for the wavelength range considered here. The contribution to the uncertainty on the responsivity is <0.02%, which is considered negligible.

2. Geometrical Parameters and Alignment

The calculation of the radiance from the reference detector signal is based on the geometrical parameters d, r_s, and r_d. The measurement uncertainty on d consists of several contributions. Distance d is obtained from two measurements. First, the distance between the sphere aperture and the flat front surface (reference plane) of the reference detector is measured with the tubular-inside micrometer. Second, the distance between the reference plane of the detector and its aperture, located about 11 mm behind the surface, is measured with a coordinate measurement machine. The sum of these distances gives d. The total uncertainty on the distance d between the apertures is estimated at 0.1 mm (standard uncertainty, k = 1), which is a combination of the uncertainty of both measurements.

The radii of both the sphere aperture and detector aperture have been measured with a coordinate measurement machine, with the following results: $r_d = 3.0087$ mm, with standard uncertainty of 0.5 µm, and $r_s = 25.297$ mm, with a standard uncertainty of 2.5 µm.

Furthermore, the sensitivity of the measured radiance to angular and lateral alignment has been quantified. We have experimentally investigated the effect of misalignment in the lateral direction by measuring the source radiance at several positions (−4 mm, −2 mm, 0 mm, +2 mm, and +4 mm displacement of the detector with respect to the optical axis). Here, the optical axis is defined by the center of the source aperture. For an estimated positioning accuracy within 2 mm of the optical axis, the deviations do not exceed 0.02%, which is considered the standard uncertainty due to lateral misalignment. The reference plane of the detector is aligned perpendicular to the optical axis using a flat mirror. The estimated residual angular misalignment is <1 mm on a 500 mm distance. The resulting change in effective diameter of the aperture is about 2×10^{-6}, which is negligible.

3. Current Measurement

The current from the photodetectors is determined from the accumulated charge Q_p and the time stamp t_p for each measurement point p and averaged:

$$i = \frac{1}{n-1} \sum_{p=1}^{p=n-1} \frac{Q_{p+1} - Q_p}{t_{p+1} - t_p}, \tag{6}$$

where n is the total number of measurement points (100). The standard deviation on the average of i is part of the measurement of the current. This is determined for each current measurement (light and dark for both reference and monitor detectors). Other uncertainty contributions to the current measurement come from the calibration of the charge meter. From the calibration of the electrometer, a deviation of −0.12% of the instrument was found. This was accounted for by correcting the measurement results with a factor C_{EM}, as mentioned above. The relative uncertainty of the electrometer for charge measurement is 0.05% (k = 1). The uncertainty on the time base is at least one order of magnitude smaller and is considered negligible.

4. Stray Light

To estimate the impact of stray light and the reproducibility of the measurement in general, the radiance calibration is performed at distances of 500 mm and 750 mm from the reference detector. This measurement is performed for a wavelength ranging from 250 nm to 950 nm and shows that the measured spectral radiance responsivity of the monitor detector agrees within 0.3% for both distances. We therefore assume stray light effects are smaller than 0.3% (rectangular distribution $k = \sqrt{3}$). Note that the differences can also have other contributions that are already accounted for, such as uncertainty on the distance measurement. Therefore, the estimate of 0.3% is considered rather conservative. This measurement also provides us with a cross check of the method and measurement model, since the radiance is calculated for two independent situations, in which the signal level at the largest distance (750 mm) is reduced by a factor of about 2.25 compared to the original distance (500 mm).

Table 1. Summary of Measurement Uncertainty of Source Radiance

Quantity	Symbol	Value	Rel. Standard Uncertainty	Sensitivity Coefficient
Detector responsivity	$R(\lambda)$	Wavelength dependent	Wavelength dependent	1
Source radius	r_s	25.297 mm	0.01%	2
Detector radius	r_d	3.0087 mm	0.02%	2
Distance	d	516.75 mm	0.02%	2
Net current ref. detector	i_{ref}	Based on $i_{ref,d}$ and $i_{ref,l}$	From measurement	1
Calibration factor electrometer	C_{EM}	1.0012	0.05%	1
Alignment effects	C_{align}	1.000	0.02%	1
Stray light	C_{stray}	1.000	0.18%	1
Net current mon. detector	$i_{mon,cal}$	based on $i_{mon,cal,d}$ and $i_{mon,cal,l}$	From measurement	1

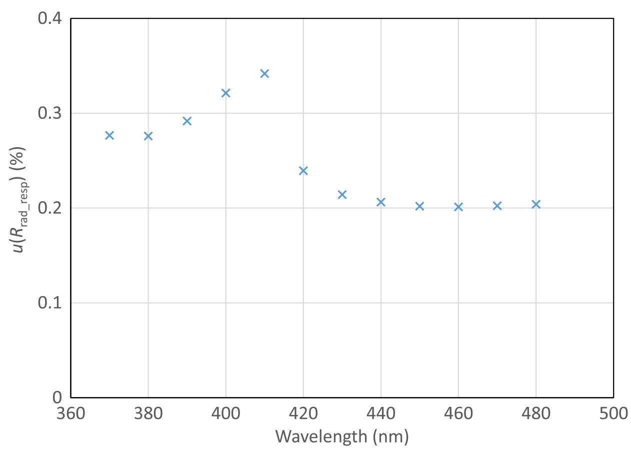

Fig. 5. Standard uncertainty on the effective spectral radiance responsivity of the monitor detector.

5. Summary of Uncertainty Contributions

In Table 1, we summarize all contributions to the measurement uncertainty on the spectral radiance responsivity calibration. Some contributions are wavelength dependent, such as the uncertainty of the effective responsivity of the monitor detector, and some contributions are based on the actual measurements, such as uncertainty on the current measurement. For the wavelength range considered in the case study below, the uncertainty of the effective spectral radiance responsivity of the monitor detector is plotted in Fig. 5.

5. VALIDATION AND CASE STUDY: TROPOLITE CALIBRATION

As a case study, we have calibrated the TROPOLITE spectroradiometer that was developed as a breadboard model for the CubeSat platform [2,6]. TROPOLITE is a hyperspectral imaging spectroradiometer developed by TNO and based on the technological heritage from Sentinel 5 P. The design emphasis was on addressing a market valuing a cost effective instrument to fit inside a 6U volume of a CubeSat for atmospheric chemistry studies. The instrument was based on an all-reflective, off-axis optical design. Commercial off-the-shelf components were used, e.g., a non-optimized grating and detector. For the current instrument model, only the spectroradiometer part was built, without an integrated telescope. A separate external telescope and aperture were installed in front of the entrance slit. The UV/VIS spectral channel of the instrument was designed to cover the spectral range from 320 nm to 500 nm, but with the current input optics, the range was limited to 370 nm to 480 nm. The spectral resolution is <0.5 nm, the spatial resolution is 0.1°, and the field of view is 60°. The TROPOLITE housing was manufactured using a relatively novel method for space hardware: 3D printing and investment casting. TROPOLITE was modified into a fully autonomous, temperature controlled, calibrated flight instrument for a flight opportunity onboard an aircraft. For details regarding the instrument design and its application as a flight model to measure NO_2 in the Berlin area, please refer to [2].

A. TROPOLITE Calibration with Tunable Radiance Source

The TROPOLITE spectroradiometer has been calibrated for spectral radiance responsivity by positioning it in front of the radiance source, replacing the reference detector in Fig. 2. The calibration of the spectroradiometer against the monitor detector was performed quasi-simultaneously. Both systems acquire data independently, while the OPO is tuned from 370 nm to 480 nm in steps of 10 nm. For each wavelength, a set of frames is acquired by the spectroradiometer, while the current from the monitor detector is measured with the electrometer. Just as for the calibration of the effective spectral radiance responsivity, the monitor detector was read every 0.5 s to acquire 100 datapoints for each measurement series.

Figure 6 shows typical measurements as obtained with the spectroradiometer during calibration. The figure is a composition of individual frames acquired for each wavelength. The integration time for 370 nm to 400 nm was 2 s. For these wavelengths the OPO beam was not attenuated. For 410 nm to 480 nm, the OPO beam was sent through an attenuator with a nominal transmission of $10^{-2.5}$, and the integration time was set at 1 s. Dark/stray light measurements were taken by blocking the transmission through the baffle (Fig. 2).

The wavelength scale of the TROPOLITE spectroradiometer is also calibrated with these measurements, since each applied wavelength is known within 0.03 nm, as verified with a laser spectrum analyzer. Based on a linear fit through the spectral calibration data, a dispersion of 0.0815 nm/pixel is found. The OPO bandwidth is about 0.1 nm, which is below the spectral resolution of the spectroradiometer (0.5 nm).

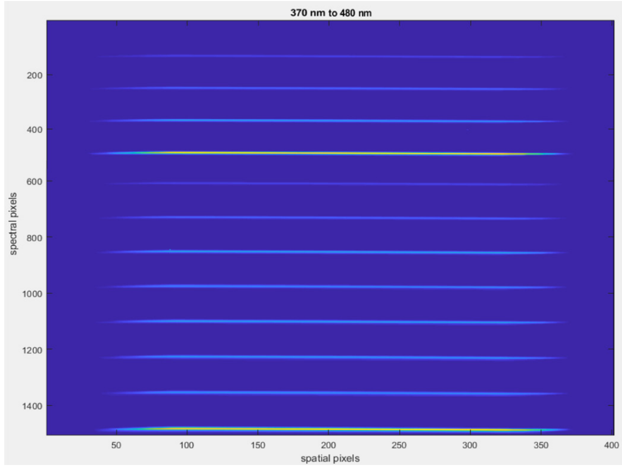

Fig. 6. Image from the TROPOLITE spectroradiometer, as obtained by combining individual images for each wavelength. The horizontal axis is the spatial axis, and the vertical axis is the spectral axis. The wavelengths range from 370 nm (top) to 480 nm (bottom).

The radiance responsivity of the spectroradiometer is determined from the calibration data as follows. First a dark-corrected average value of the spectral signal is determined for each wavelength based on the dark and light frames available for this wavelength. From each measured frame, five lines are analyzed, corresponding to five neighboring spatial pixels in the center of the field of view. The average signal is determined by averaging over the five spatial pixels and the available frames (about 100 per wavelength). Subsequently, the total number of counts per second [expressed in binary units (BU)/s] is determined by integrating the signal over the illuminated spectral pixels and normalizing with the integration time. The radiance of the source is based on the measured current of the monitor detector and the effective spectral responsivity as determined in Section 4. Based on the total number of counts and the radiance of the source, the radiance responsivity of the spectroradiometer is determined, expressed in the units $(\mathrm{BU\ s^{-1}})/(\mathrm{W\ m^{-2} sr^{-1}})$.

The measurement uncertainty of the spectral radiance responsivity consists of several contributions. These comprise the standard uncertainty on the reference radiance source (Fig. 5), an estimated standard uncertainty of 0.1% for the alignment of TROPOLITE with respect to the sphere aperture, and 0.1% for monitor detector noise (both wavelength independent). In addition, a significant contribution can be attributed to statistical fluctuation of the TROPOLITE signal measurement, which ranges from about 0.1% to 0.8%. The results and uncertainties will be compared to those obtained via the classical traceability route with an FEL lamp combined with a diffuser, as discussed in the next section.

B. Validation of the Results

To validate the laser-based method, a traditional calibration of the TROPOLITE instrument has been performed with an FEL lamp and a diffuser with the setup schematically shown in Fig. 7. The FEL lamp was calibrated by VSL for spectral irradiance with an uncertainty of 2% to 3% ($k = 2$, wavelength dependent). To convert the lamp irradiance into radiance, a diffuser is used, which is positioned at a well-defined distance from the

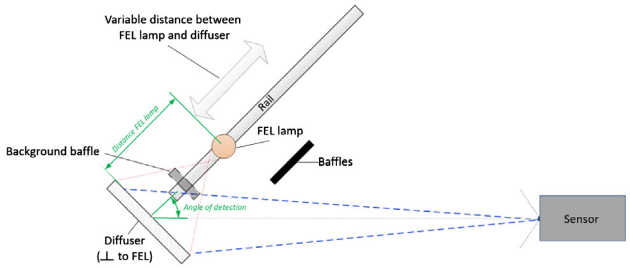

Fig. 7. Schematic of setup for calibrating a spectroradiometer for radiance with an FEL lamp and diffuser.

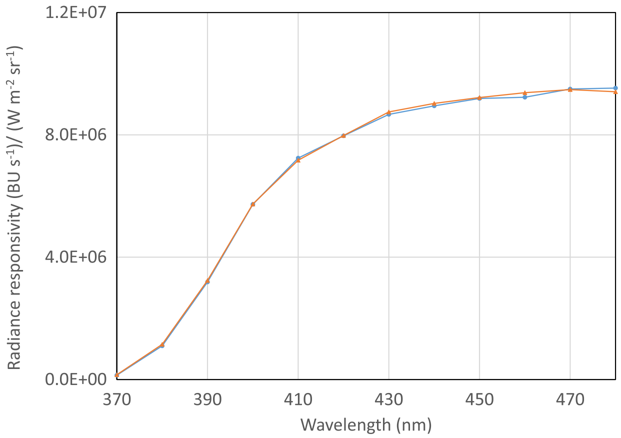

Fig. 8. Spectral radiance responsivity of TROPOLITE as measured with an FEL lamp positioned at 75 cm from the diffuser (orange triangles) and with the OPO-based radiance source (blue dots).

lamp. The diffuser has been applied for several satellite instrument calibrations, and its bidirectional scattering distribution function (BSDF) has been thoroughly characterized. Both the diffuser calibration and the calibration of TROPOLITE have been performed in the $R(0°/45°, \lambda)$ geometry.

The results of the calibration of the spectral radiance responsivity with both methods are shown in Fig. 8. Here, the radiance from the FEL lamp–diffuser combination has been determined for a 75 cm distance between lamp and diffuser. The ratio of the responsivities as measured with the two methods is plotted in Fig. 9. As can be observed from the results, both methods agree within 2% for 390 nm to 480 nm. Only for 360 nm and 370 nm do the results deviate more. Here, the responsivity of the sensor is very low. The low responsivity combined with the very low emission of the FEL lamp in the UV wavelength range gives rise to small signal-to-noise ratios for the FEL calibration, leading to an increasing uncertainty in this region. The uncertainty budget for the FEL–diffuser calibration comprises several contributions. The standard uncertainty on the reference FEL lamp ranges from about 1% − 1.5%. The uncertainty of the BSDF calibration is 0.15%–0.21%. Furthermore, there is an uncertainty contribution from the geometrical alignment of the FEL lamp and diffuser (0.4%) and alignment of the spectroradiometer (0.1%). For the blue side of the spectrum, spectral stray light plays an important role, since both responsivity and applied signal are low for these wavelengths. Spectral stray light is estimated to be 14% at 370 nm ($k = 1$), dropping rapidly for

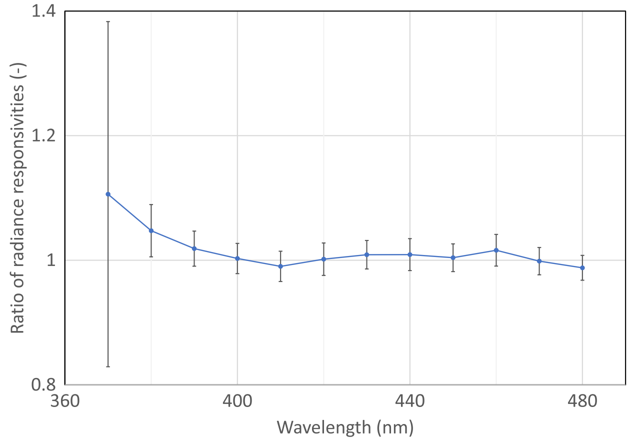

Fig. 9. Ratio between the radiance responsivity of TROPOLITE as measured with FEL–diffuser source and the OPO-based radiance source. The uncertainty bars show the $k = 2$ measurement uncertainty of the ratio.

Table 2. Standard Uncertainty of Calibration of the TROPOLITE Spectroradiometer for Calibration with an OPO and with an FEL Lamp[a]

Wavelength nm	Uncertainty OPO ($k = 1$)%	Uncertainty FEL ($k = 1$)%	Uncertainty Ratio ($k = 2$)%
380	0.34	13.85	27
390	0.85	1.92	4.2
400	0.76	1.19	2.8
410	0.47	1.12	2.4
420	0.54	1.09	2.4
430	0.76	1.06	2.6
440	0.48	1.04	2.3
450	0.79	1.01	2.6
460	0.47	1.01	2.2
470	0.78	1.00	2.5
480	0.48	0.98	2.2
380	0.28	0.96	2.0

[a]In the right-hand column, the combined uncertainty is shown ($k = 2$).

longer wavelengths. An overview of the measurement uncertainties of both methods is provided in Table 2. The combined uncertainty provided is the uncertainty on the ratio of both measurements and is also shown as error bars in Fig. 9.

In Table 2, it is observed that the uncertainty on the calibration of the radiance responsivity is smaller for the OPO-based method. A significant contribution for this method comes from the calibration of the spectroradiometer itself and is assigned to instability of the OPO output in combination with imperfect synchronization between TROPOLITE and charge meter measurement. Further reduction of the uncertainty, down to about 0.5% for all wavelengths ($k = 1$), is expected to be achievable by extending the measurement time and improving the synchronization between the TROPOLITE data acquisition and the charge meter measurement. For the FEL-based method, there is little room for further improvement, since the measurement uncertainty is limited by the calibration of the reference lamp.

6. CONCLUSION

We have demonstrated the calibration of the spectral radiance responsivity of a CubeSat spectroradiometer in the UV/VIS wavelength range with a narrow-band, widely tunable radiance source. The radiance source consists of an OPO coupled to an integrating sphere. Radiance of the source is traceable to SI via a calibrated reference detector and geometrical measurements. The results have been compared to a calibration with an FEL reference lamp and a diffuser. The measurement results agree within the combined measurement uncertainty, which provides a validation of the OPO-based method. The expanded measurement uncertainty ($k = 2$) for the OPO-based method varies from about 0.6% to 1.7% for the wavelength range of 370 nm to 480 nm, with room for further reduction of the uncertainty to <1% for the full wavelength range by extending the calibration time and improving synchronization. The presented method may lead to overall reduction of calibration time and cost. It not only provides calibration for spectral radiance responsivity at a reduced measurement uncertainty, but also additional information that could be used for further characterization of the spectroradiometer that would require additional efforts for the lamp-based approach. For example, the calibration of the wavelength scale of the spectroradiometer is automatically provided from the set OPO wavelength. Furthermore, the application of a narrow-band and tunable source allows for implementation of spectral stray light correction [7]. The large tuning range of the source also allows for characterization of out-of-band stray light [8].

Funding. European Metrology Programme for Innovation and Research (16ENV03).

Acknowledgment. The authors thank Gerard Kotte for calibrating the apertures and Roland van Bemmelen for calibrating the electrometers. This work was executed as part of the Metrology for Earth Observation and Climate project (MetEOC-3).

Disclosures. SvdB, PD: VSL B.V. (E). GO, MPP, ND: the authors declare no conflicts of interest.

REFERENCES

1. Y. Zong, S. W. Brown, G. P. Eppeldauer, K. R. Lykke, and Y. Ohno, "A new method for spectral irradiance and radiance responsivity calibrations using kilohertz pulsed tunable optical parametric oscillators," Metrologia **49**, S124 (2012).
2. B. De Goeij, G. Otter, J. Van Wakeren, J. Veefkind, T. Vlemmix, X. Ge, P. Levelt, B. Dirks, P. Toet, L. van der Wal, and R. Jansen, "First aircraft test results of a compact, low cost hyperspectral imager for earth observation from space," Proc. SPIE**10562**, 105621N (2017).
3. S. van den Berg, P. Dekker, T. van der Laan, G. Otter, N. Dijkhuizen, B. Gür, and S. Brinkers, "Traceable radiance source for spectroradiometer calibration," Proc. SPIE **11180**, 2238–2247 (2019).
4. A. Gaertner, "Optical radiation measurement," in *Modern Metrology Concerns* (2012), pp. 223–262.
5. C. Schrama, P. Bloembergen, and E. Van der Ham, "Monochromator-based cryogenic radiometry between 1 μm and 20 μm," Metrologia **37**, 567 (2000).
6. L. Maresi, W. V. D. Meulen, and R. Vink, "TROPOLITE, on the path of atmospheric chemistry made simple," Proc. SPIE **9241**, 128–138 (2014).
7. Y. Zong, S. W. Brown, B. C. Johnson, K. R. Lykke, and Y. Ohno, "Simple spectral stray light correction method for array spectroradiometers," Appl. Opt. **45**, 1111–1119 (2006).
8. S. Nevas, J. Gröbner, L. Egli, and M. Blumthaler, "Stray light correction of array spectroradiometers for solar UV measurements," Appl. Opt. **53**, 4313–4319 (2014).